

BRIGHTNESS OF AN INTENSE ELECTRON BEAM GENERATED BY A PULSE-LASER IRRADIATED PHOTOCATHODE<sup>a</sup>

P.E. Oettinger and I. Bursuc, Thermo Electron Corporation,  
85 First Avenue, Waltham, MA 02254  
R.E. Shefer, Science Research Laboratory,  
15 Ward St., Somerville, MA 02143  
E. Pugh, Physical Sciences Incorporated,  
Research Park, Andover, MA 01810

ABSTRACT

Linac-driven free electron lasers, new powerful synchrotron radiation sources, and advanced high-power microwave devices all require very bright emitters of electrons to operate efficiently. By irradiating a Cs<sub>3</sub>Sb photocathode with a frequency-doubled Nd:glass laser, we have obtained a very high normalized electron beam brightness of over 10<sup>11</sup> A/m<sup>2</sup>/rad<sup>2</sup>. Peak currents emitted from the 1-cm<sup>2</sup> surface in 50-ns pulses ranged up to 80 A. Measured normalized emittances were between 5 and 9 π-mm-mrad.

The efficient transfer of beam energy into the radiative field of free electron lasers, synchrotron sources, and powerful microwave tubes requires electron beams of very high brightness. This paper presents experimental data on the high brightness achievable from photoemitted beams generated by pulse-laser-irradiating a cesium antimonide (Cs<sub>3</sub>Sb) surface.

In accordance with accepted practice,<sup>1</sup> B<sub>n</sub> is defined as:

$$B_n = \frac{I}{\pi^2 \epsilon_n^2} \quad (1)$$

where I is the beam current. For a beam propagating in the z-direction, the normalized emittance ε<sub>n</sub> is given by:

$$\epsilon_n = \beta \gamma \frac{A}{\pi} \quad (2)$$

where β = v<sub>z</sub>/c, γ = (1 - β<sup>2</sup>)<sup>-1/2</sup> and A is the area in transverse phase space occupied by the beam. Using the approximation A ≈ r<sub>c</sub><sup>2</sup>π<θ>, where r<sub>c</sub> is the cathode radius and <θ> is an average ratio of transverse-to-longitudinal electron momenta, equation 2 can be rewritten as:

$$\epsilon_n \approx r_c \left( \frac{2 E_{\perp}}{m_0 c^2} \right)^{1/2} \quad (3)$$

E<sub>⊥</sub> is the average electron transverse energy at the cathode surface and can be considered to be a measure of the transverse energy spread of the beam. Transverse energies of approximately 0.2 eV have

been reported from field-retarding parallel plate energy analyses of very low current density (up to 10 μA/cm<sup>2</sup>) beams emitted by Cs<sub>3</sub>Sb photoemissive surfaces exposed to cw 514.5 nm argon ion laser radiation.<sup>2</sup> In the present experiments, this energy spread was measured at much higher current densities, and the associated photosource brightness was determined. The irradiating source was a frequency-doubled, Q-switched Nd:glass laser emitting 50 ns (FWHM) pulses at a wavelength of 532 nm. DC breakdown limited the currents to 80 A from a 1 cm<sup>2</sup> photocathode; values of over 200 A have previously been reported from this cathode material.<sup>3</sup>

Cs<sub>3</sub>Sb is a positive electron affinity photoemissive material, which is relatively easy to fabricate. At 532 nm, commercial tube cathodes typically have a quantum efficiency of 4 percent. The quantum efficiencies of the photosurfaces used in these experiments, measured under operating conditions, generally ranged from 1 to 3 percent.

Tests were performed using the apparatus shown in Figure 1a. With the vacuum chamber maintained at a pressure of 10<sup>-9</sup> torr, a Cs<sub>3</sub>Sb photoemissive surface was fabricated in situ. A current lead from the photocathode passed to ground through an insulated feedthrough in the vacuum chamber wall, with the pulsed current detected by a Pearson current probe surrounding this lead. The anode consisted of a 1-mil-thick planar molybdenum pepperpot foil, spaced 6 to 7 mm from the cathode, followed by a 14-cm long, field-free drift region terminating at a 5-cm-diameter quartz disc. The quartz was coated on the inside by a P-1 (Zn<sub>2</sub>SiO<sub>4</sub>:Mn) phosphor overcoated with a 200 nm layer of aluminum. The phosphor screen was photographed through a port at the far end of the vacuum chamber. Five 1-mil-diameter holes in the pepperpot were configured into a cross, with the outside four holes equally spaced 3 mm from a central axial hole. DC voltages of up to 55 kV were applied to the anode, with a 300 pF cable supplying the charge to the diode. Temporally resolved traces of the photocurrent, and time integrated photographs of the beamlet images on the phosphor screen, were simultaneously recorded.

Beam emittance was determined by measuring the size of the beamlet images. The envelope of the expansion of a single beamlet is shown schematically in Figure 1b. Ideally, the intensity profiles of the beamlets after they traverse the field-free drift space should be a measure of the distribution of transverse velocities in the electron beam at the pepperpot disc. This distribution of transverse velocities, along with a knowledge of the beam current density profile, can then be used to determine the area in transverse phase space occupied by the beam, and thus to calculate its emittance.<sup>4,5</sup> In the experiments, it was

<sup>a</sup>Work supported in part by the Los Alamos National Laboratory under Contract No. 9-X54-M3489-1 and in part by corporate funds of Thermo Electron Corporation.

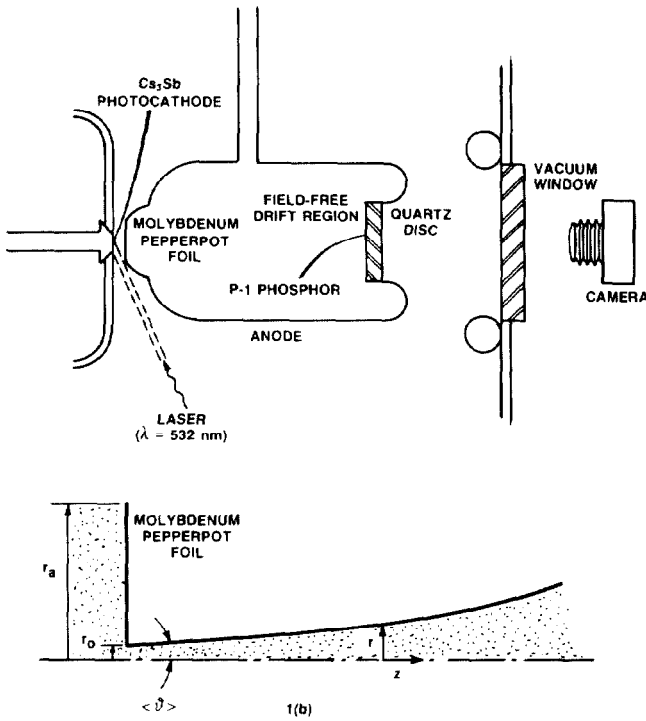


Figure 1. Experimental Apparatus (1a) and the Envelope of the Expanding Beamlet in the Field-Free Drift Region (1b)

generally observed that the beamlet images were all approximately the same in size and intensity (Figure 2). Therefore, it was assumed that both the current density and transverse velocity distributions were independent of radial position in the beam, and the emittance could be determined from any one imaged beamlet. In addition, the beamlet images on the film were saturated, so that the spot diameters measured directly from the film positives yielded upper limits on the width of the distribution of the transverse angles in the beam. Thus, the measurements reported herein represent an upper bound on the true emittance of the photoelectron beam.



Figure 2. Images of 1-mil-diameter Pepperpot Holes on P-1 Phosphor Screen for an Applied Voltage of 50 kV

In addition to the emittance, the size of the beamlet images was affected by the diode optics and the electron space charge in the drift region. The electrostatic and self-magnetic fields in the anode-cathode gap caused a radial distribution of transverse electron velocities across the beam, and thus across each pepperpot aperture. The magnitude of this effect was determined by using the SLAC electron optics code<sup>6</sup> to calculate the particle trajectories within the diode for the conditions of the experiments. The results indicated that, for the pepperpot used, such velocity distributions accounted for less than a 10 percent contribution to a beamlet radius at the phosphor screen.

The size of a beamlet image was also affected by the space charge fields in the field-free drift region,<sup>7</sup> and by defocussing of the beamlet at the pepperpot aperture.<sup>8</sup> The contribution to image size from these effects was calculated by solving the envelope equation<sup>7</sup>

$$\frac{d^2 r}{dz^2} - \frac{K}{r} - \frac{\epsilon_b^2}{r^3} = 0 \quad (4)$$

for an individual beamlet in the field-free drift region. Here  $r$  and  $z$  denote the radial and axial coordinates of the beamlet envelope. The second and third terms in equation 4 represent the expansion of the envelope due to space charge and beamlet emittance,  $\epsilon_b$  respectively. For a weakly relativistic beam,

$$K = \frac{e j_0 r_0^2}{2 \epsilon_0 m_0 (\gamma \beta c)^3} \quad (5)$$

where  $j_0$  is the beam current density at the pepperpot, and  $r_0$  is the radius of a pepperpot aperture. The beamlet emittance is related to the normalized beam emittance by

$$\epsilon_b = \frac{\epsilon_n r_0}{\beta \gamma r_a} \quad (6)$$

where  $r_a$  is the radius of the full beam in the diode at the pepperpot disc. Beamlet defocussing at the pepperpot aperture ( $z = 0$ ) was introduced in the solution of equation 6 as a boundary condition

$$\left( \frac{dr}{dz} \right)_{z=0} = \frac{r_0}{nD} \quad (7)$$

where  $D$  is the diode spacing, and  $n$  has a value between 3 and 4, depending on whether the emission is space charge limited or not.

For assumed values of  $\epsilon_n$ , the expected image size of the beamlets was numerically calculated from equation 4 subject to the boundary condition of equation 7. By comparing the calculated and measured image sizes, the actual value of  $\epsilon_n$  was determined.

The relative contributions of emittance, aperture defocussing and space charge to the size of a beamlet image at the phosphor screen can be estimated from the integral of equation 4. Far from the pepperpot aperture, where  $r \gg r_0$ ,

$$\left( \frac{dr}{dz} \right)^2 \approx \left( \frac{r_0}{nD} \right)^2 + 2K \ln \left( \frac{r}{r_0} \right) + \left( \frac{1}{\beta \gamma} \frac{\epsilon_n}{r_a} \right)^2 \quad (8)$$

The three terms on the right hand side of equation 8 will be recognized as the sum of the squares of the

beamlet expansion angles due to aperture defocussing  $(\theta_f)^2$ , space charge  $(\theta_{sc})^2$ , and emittance  $(\theta_{\epsilon_b})^2$  respectively. For the parameters of this experiment,  $(\theta_{\epsilon_b})^2 > 2 (\theta_{sc})^2 > 4 (\theta_f)^2$  at the phosphor screen, so that the beamlet expansion was always emittance dominated.

The normalized beam brightness, calculated from equation 1, is plotted as a function of current in Figure 3. Error bars indicate the experimental uncertainty in measuring the image sizes. The dashed curves represent brightnesses corresponding to normalized beam emittances of 5 and 8.7  $\pi$ -mm-mrad. For this range of  $\epsilon_n$ , into which most of the experimental data fall,  $E_{\perp}$  at the photocathode varies according to equation 3, between 0.2 and 0.6 eV.

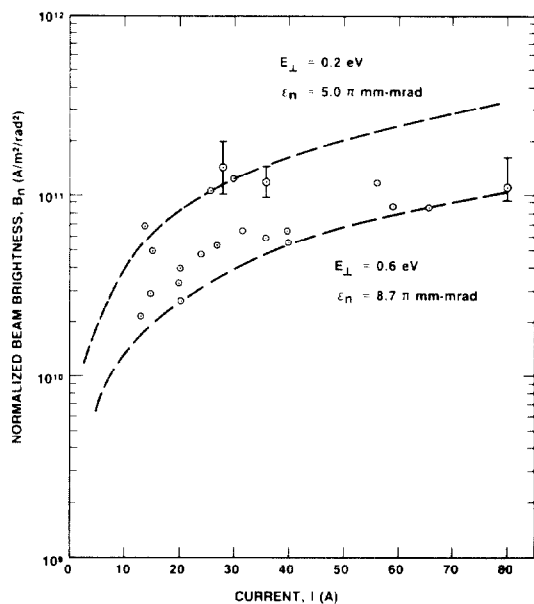


Figure 3. Normalized Brightness as a Function of Current Generated from a  $1 \text{ cm}^2$   $\text{Cs}_3\text{Sb}$  Photocathode Irradiated by a 50 ns Long Laser Pulse at a Wavelength of 532 nm

These values are reasonably consistent with the difference between the frequency-doubled laser photon energy and that energy (band gap plus electron affinity) needed to eject an electron from the  $\text{Cs}_3\text{Sb}$  surface,<sup>9</sup> and are in general agreement with the low-current results reported in Reference 2. Thus, Figure 3 indicates that the transverse energy spread of the photocathode beam remains nearly constant for current densities up to at least  $80 \text{ A/cm}^2$ , and that a corresponding beam brightness of the order of  $10^{11} \text{ A/m}^2/\text{rad}^2$  can be achieved. Such a normalized brightness is nearly an order of magnitude greater than currently observed in operational accelerators (Figure 4).

Because very short pulses are expected to cause substantial growth in beam emittance, a preliminary series of experiments was performed using 100-ps long, frequency-doubled Q-switched pulses from a Nd:YAG laser. The patterns observed for current densities estimated to be 5 to  $10 \text{ A/cm}^2$  showed no significant increase in spot size over those recorded for the previous 50-ns pulses, suggesting no major change in transverse photoelectron energy spread. If this low energy spread can be maintained as the current density is increased to  $200 \text{ A/cm}^2$  and as the pulse length is reduced further to 60 ps, the photocathode beam will more than meet the requirements of the next generation of large rf-driven free electron lasers.<sup>10</sup>

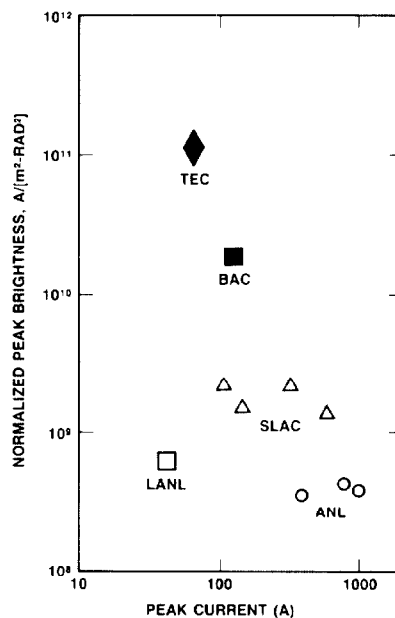


Figure 4. Normalized Brightness of Laser-Driven Photocathode at 80 A (Thermo Electron Corp. [TEC]) and Subharmonic Buncher Systems in Single Bunch Accelerators (Argonne National Laboratory [ANL], Stanford Linear Collider [SLC]) and Pulse-Comb Accelerators (Boeing Aerospace Co. [BAC], Los Alamos National Laboratory [LANL])

The authors wish to thank Mr. John Fronduto for help with the experiments, Dr. Alfred Sommer for advice on photocathodes, and Dr. Milan Tekula for assistance with the computer analyses.

#### REFERENCES

1. C.W. Roberson, J.A. Pasour, F. Mako, R.F. Luce, Jr., and P. Sprangle, *Infrared and Millimeter Waves*, Vol. 10, Chapt. 7, Academic Press, 1983, pp. 361-398.
2. C.H. Lee, *J. Appl. Phys.* **54**, 4578 (1983).
3. C. Lee, P.E. Oettinger, E.R. Pugh, R. Klinkowstein, J.H. Jacobs, R.L. Sheffield and J. Fraser, *IEEE Trans. Nucl. Sci.* **NS-32**(5), 3045 (1984).
4. C. Lejeune and J. Aubert, in *Applied Charged Particle Optics*, ed. A. Septier (Academic Press, New York, 1980), Part A, pp. 159-259.
5. D.A. Kirkpatrick, R.E. Shefer, and G. Bekefi, *J. Appl. Phys.* **57**, 5011 (1985).
6. W.B. Herrmannsfeldt, Electron Trajectory Program, SLAC Report #226, Nov. 1979.
7. J.D. Lawson, in *Applied Charged Particle Optics*, ed. A. Septier (Academic, New York, 1983), Part C, pp. 2-47.
8. K.R. Spangenberg, *Vacuum Tubes* (McGraw-Hill), New York, 1948) p. 354.
9. A. Sommer, *Photoemissive Materials*, John Wiley, New York (1968) p. 10.
10. J.S. Fraser, R.L. Sheffield, E.R. Gray, and G.W. Rodenz, *IEEE Trans. Nucl. Sci.* **NS-32**(5), 1791 (1985).